Ionic Conductivity of the Aqueous Layer Separating a Lipid Bilayer Membrane and a Glass Support †

ARTICLE *in* LANGMUIR · JANUARY 2007

Impact Factor: 4.46 · DOI: 10.1021/la061457a · Source: PubMed

7 AUTHORS, INCLUDING:

Ryan J White
University of Maryland, Baltimore County
44 PUBLICATIONS **1,510** CITATIONS
SEE PROFILE

Eric N Ervin
Electronic Biosciences, INC
19 PUBLICATIONS **582** CITATIONS
SEE PROFILE

Ionic Conductivity of the Aqueous Layer Separating a Lipid Bilayer Membrane and a Glass Support†

Ryan J. White,‡ Bo Zhang,‡ Susan Daniel,§ John M. Tang,|| Eric N. Ervin,‡ Paul S. Cremer,*,§ and Henry S. White*,‡

Department of Chemistry, University of Utah, 315 S. 1400 E, Salt Lake City, Utah 84112, Department of Chemistry, Texas A&M University, P.O. Box 30012, College Station, Texas 77842-3012, and Department of Molecular Biophysics and Physiology, Rush University Medical Center, 1750 W. Harrison Street, Chicago, Illinois 60612

Received May 23, 2006. In Final Form: July 12, 2006

The in-plane ionic conductivity of the ∼1-nm-thick aqueous layer separating a 1-palmitoyl-2-oleoyl-*sn*-glycero-3-phosphocholine (POPC) bilayer membrane and a glass support was investigated. The aqueous layer conductivity was measured by tip-dip deposition of a POPC bilayer onto the surface of a 20- to 75-μm-thick glass membrane containing a single conical-shaped nanopore and recording the current−voltage ($i-V$) behavior of the glass membrane nanopore/POPC bilayer structure. The steady-state current across the glass membrane passes through the nanopore (45−480 nm radius) and spreads radially outward within the aqueous layer between the glass support and bilayer. This aqueous layer corresponds to the dominant resistance of the glass membrane nanopore/POPC bilayer structure. Fluorescence recovery after photobleaching measurements using dye-labeled lipids verified that the POPC bilayer maintains a significant degree of fluidity on the glass membrane. The slopes of ohmic $i-V$ curves yield an aqueous layer conductivity of $(3 \pm 1) \times 10^{-3}\ \Omega^{-1}\ \mathrm{cm}^{-1}$ assuming a layer thickness of 1.0 nm. This conductivity is essentially independent of the concentration of KCl in the bulk solution (10^{-4} to 1 M) in contact with the membrane. The results indicate that the concentration and mobility of charge carriers in the aqueous layer between the glass support and bilayer are largely determined by the local structure of the glass/water/bilayer interface.

Introduction

A thin aqueous layer resides between a lipid bilayer and a solid support (e.g., glass, quartz, or gold) and acts as a lubrication layer for the 2D fluid layer of lipid molecules adjacent to it. In investigations of lipid bilayers on quartz and glass, Tamm and McConnell initially proposed the existence of the aqueous layer based on observations of the rapid diffusion of fluorescently tagged lipids in the supported membrane.[1] Subsequently, several experimental investigations using different methods (e.g., NMR,[2] neutron reflectivity[3−6] and atomic force microscopy[4]) have reported values for the thickness of the aqueous layer ranging from 0.6 to 3 nm, with most values clustering around ∼1 nm. The equilibrium thickness of the aqueous layer is determined by electrostatic, van der Waals, and hydration forces, and has been calculated to be on the order of ∼1 nm.[7]

In this report, we describe measurements of the in-plane ionic conductivity of the aqueous layer between a 1-palmitoyl-2-oleoyl-*sn*-glycero-3-phosphocholine (POPC) bilayer membrane and a glass support. Measurement of the ion conductivity is anticipated to shed light on the motion of ions and H_2O molecules within the thin aqueous layer, providing fundamental insight into the nature of this region. Specifically, ionic conductivity reflects the product of the mobility and concentration of charge-carrying ions, properties of the aqueous layer that will be strongly influenced by electrostatic and structural factors associated with the glass/water/bilayer interface.

Theoretical and experimental investigations of the dynamic motion and structure of water in nanopores, in confined layers, and at interfaces suggest that water immediately adjacent to charged or hydrophilic surfaces is more highly ordered with significantly increased viscosity.[8−16] Most relevant to the present report, Osman and co-workers previously measured the in-plane conductivity of the ∼4-nm-thick aqueous "ionic reservoir" between a Au substrate and a tethered bilayer membrane.[17] Their results indicate that the ion mobilities of alkali and chloride ions in this layer are 3 to 4 orders of magnitude lower than in bulk solution, a finding attributed to increased ion pair formation associated with a lower dielectric constant of the confined aqueous layer. In related work, Unwin and co-workers[18,19] demonstrated that the motion of protons parallel to acidic and zwitterionic Langmuir monolayers deposited at the air/water interface is

† Part of the Electrochemistry special issue.

* Corresponding authors. E-mail: cremer@mail.chem.tamu.edu; white@chem.utah.edu.

‡ University of Utah.

§ Texas A&M University.

|| Rush University Medical Center.

(1) Tamm, L. K.; McConnell, H. M. *Biophys. J.* **1985**, *46*, 105.
(2) Bayerl, T. M.; Bloom, M. *Biophys. J.* **1990**, *58*, 357.
(3) Johnson, S. J.; Bayerl, T. M.; McDermott, D. C.; Adam, G. W.; Rennie, A. R.; Thomas, R. K.; Sackmann, E. *Biophys. J.* **1991**, *59*, 289.
(4) Koenig, B. W.; Krueger, S.; Orts, W. J.; Majkrzak, C. F.; Berk, N. F.; Silverton, J. V.; Gawrisch, K. *Langmuir* **1996**, *12*, 1343.
(5) Charitat, T.; Bellet-Amalric, E.; Fragneto, G.; Graner, F. *Eur. Phys. J. B* **1999**, *8*, 583
(6) Gutberlet, T.; Steitz, R.; Fragneto, G.; Klosgen, B. *J. Phys.: Condens. Matter* **2004**, *16*, S2469.
(7) Cremer, P. S.; Boxer, S. G. *J. Phys. Chem. B* **1999**, *103*, 2554.
(8) Bellissent-Funel, M.-C. *J. Phys.: Condens. Matter* **2001**, *13*, 9165.
(9) Gragson, D. E.; McCarty, B. M.; Richmond, G. L. *J. Am. Chem. Soc.* **1997**, *119*, 614.
(10) Watry, M. R.; Tarbuck, T. L.; Richmond, G. L. *J. Phys. Chem. B* **2003**, *107*, 512.
(11) Yalamanchili, M. R.; Atia, A. A.; Miller, J. D. *Langmuir* **1996**, *12*, 4176.
(12) Scodinu, A.; Fourkas, J. T. *J. Phys. Chem. B* **2002**, *106*, 10292.
(13) Boissiere, C.; Brubach, J. B.; Mermet, A.; de Marzi, G.; Bourgaux, C.; Prouzet, E.; Roy, P. *J. Phys. Chem. B* **2002**, *106*, 1032.
(14) Qiao, R.; Aluru, N. R. *Langmuir* **2005**, *21*, 8972.
(15) Mashl, R. J.; Joseph, S.; Aluru, N. R.; Jakobsson, E. *Nano Lett.* **2003**, *3*, 589.
(16) Schmitz, K. S. *J. Phys. Chem. B* **1999**, *103*. 8882.
(17) Krishna, G.; Schulte, J.; Cornell, B. A.; Pace, R. J.; Osman, P. D. *Langmuir* **2003**, *19*, 2294.
(18) Zhang, J.; Unwin, P. R. *J. Am Chem. Soc.* **2002**, *124*, 2379−2383.
(19) Slevin, C. J.; Unwin, P. R. *J. Am. Chem. Soc.* **2000**, *122*, 2597−2602.

10.1021/la061457a CCC: $33.50
Published on Web 08/22/2006

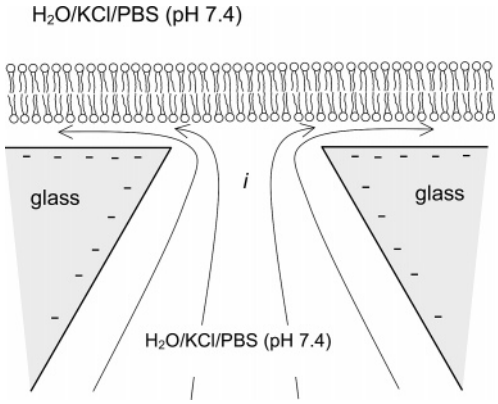

Figure 1. Schematic drawing of a supported POPC bilayer membrane spanning the orifice of a nanopore in a glass membrane. The solutions on the opposite sides of the glass membrane contain equal concentrations of KCl and are buffered to pH 7.4. The least-resistive path of current is in the water layer between the bilayer membrane and the glass surface.

significantly influenced by chemical and electrostatic interactions. Similarly, the dynamic motion of ions in an ~1-nm-thick layer of water that is strongly confined between a glass surface and a fluid lipid bilayer is expected to be very different from the dynamic motion of the same ions in free solution.

As schematically depicted in Figure 1, our methodology for measuring conductivity is based on depositing a lipid bilayer on a thin (20 to 75 μm) glass membrane that contains a single conical-shaped pore. Applying a voltage across the glass membrane (using reversible Ag/AgCl electrodes) results in the migration of ions through the conical pore to the glass/bilayer interface. At the opening of the pore, ion migration follows the path of least resistance, which corresponds to the water layer between the bilayer and glass. As the ions enter this aqueous layer, they spread radially outward from the pore orifice, eventually exiting the aqueous layer at the edge of the bilayer film. As will be experimentally demonstrated in this report, because the spreading resistance of the 1-nm-thick aqueous layer (~5 GΩ) is measured to be much larger than that of the conical-shaped pore (~5 MΩ), the experimentally measured resistance corresponds almost entirely to the aqueous layer. Simple geometrical relationships and Ohm's law allow the measured resistance to be converted to the ionic conductivity of the aqueous layer.

In addition to reporting the methodology for measuring ion conductivity, we demonstrate that the conductivity of the aqueous layer is essentially independent of the KCl concentration of the solution in contact with the supported bilayer for KCl concentrations between 10^{-4} and 1.0 M. This result suggests that the surface density of K^+ in the aqueous layer is largely determined by the surface density of deprotonated silanol groups on the glass surface and that "free" K^+ and Cl^- are largely excluded from this region. The magnitude of the conductivity also suggests that the ion mobility of charge-carrying K^+ is 2 to 3 orders of magnitude smaller that in bulk aqueous solution, consistent with the notion that the movement of ions and molecules within this layer is dominated by interactions with the confining surfaces.

Experimental Section

Materials. KCl, K_2HPO_4, and KH_2PO_4 (Mallinckrodt) were used as received. All aqueous solutions were prepared using water of at least 18 MΩ cm resistivity from a Barnstead E-pure water purification system. The phospholipid, 1-palmitoyl-2-oleoyl-*sn*-glycero-3-phosphocholine (POPC), was purchased from Avanti Polar Lipids (Alabaster, AL). *N*-(Texas Red sulfonyl)-1,2-dihexadecanoyl-*sn*-glycero-3-phosphoethanolamine (Texas Red DHPE) was purchased from Molecular Probes (Eugene, OR).

Glass Membrane and Nanopore. Glass membranes containing a single conical-shaped nanopore were constructed following a previously published procedure for preparing conical-shape Pt nanopore electrodes.[20] In brief, a 25-μm-diameter Pt wire is electrochemically etched to produce a sharp cone-shaped tip with a half-cone angle, θ, of 10 ± 1°. A short length (20 to 75 μm) of the sharpened end of the Pt wire is sealed in the end of a glass capillary (Dagan Corp., Prism glass capillaries, SB16, 1.65 mm outer diameter, 0.75 mm inner diameter, soda lime) using a hydrogen/air torch. The sealed end of the capillary is polished flat to produce a Pt disk electrode shrouded in glass. The exposed Pt surface is then electrochemically etched by applying a 2 V, 60 Hz sine wave in a $CaCl_2$ solution. This etching step produces a conical-shaped pore in the glass, with a Pt microdisk located at the pore base. Details of the sharpening, sealing, polishing, and etching have been previously described.[20] Following preparation of the Pt nanopore electrode, the remaining Pt wire is removed from the pore by gently pulling it from the glass membrane. We hereafter refer to this structure as a glass membrane nanopore.

The pore length (20−75 μm) and large opening radius were measured by optical microscopy. The radius of the small opening of the pore, r_1, was measured by two methods. In the first, we use the fact that r_1 is equal to the radius of the Pt disk prior to etching the Pt. The radius of the Pt disk is determined by measuring the steady-state voltammetric limiting current for the oxidation of ferrocene in an unstirred acetonitrile solution. The limiting current is given by $i_d = 4nFDC^*r_1$, where $n = 1$ electron per molecule, F is Faraday's constant, and D and C^* are, respectively, the diffusion coefficient (2.4×10^{-5} cm^2 s^{-1}) and solution concentration of ferrocene.[21] In the second method, the resistance of the pore (after removal of the Pt) was measured in a 1 M KCl solution by recording the current through the pore in response to a voltage applied between two reversible Ag/AgCl electrodes. The resistance of a truncated conical-shaped pore comprises the internal resistance of the pore (R_{in}) and the external resistance that spreads radially outward from the pore opening (R_{ex}). For half-cone angles of less that 20°, the overall resistance is given by[20]

$$R_p = R_{in} + R_{ex} = \frac{L}{\pi\kappa_{bulk} r_1 (r_1 + L \tan\theta)} + \frac{1}{4\kappa_{bulk} r_1} \qquad (1)$$

where κ_{bulk} is the conductivity of the bulk KCl solution. As previously shown, for $L \gg r_1$, the pore resistance is a function of only r_1 and θ.[20] Under these conditions, eq 1 reduces to eq 2.

$$R_p = \frac{1}{\kappa r_1}\left(\frac{1}{\pi \tan\theta} + \frac{1}{4}\right) \qquad (2)$$

The condition that $L \gg r_1$ is fulfilled for the membranes used in these investigations, as $L = 20-75$ μm and the largest value of r_1 is 480 nm (most values of r_1 in this report are significantly smaller). In addition, because $\theta = 10°$ (±1° by optical microscopy), eq 2 can be simplified and rearranged to yield the pore orifice radius r_1 (cm) in terms of the resistance R_p in a 1 M KCl solutions ($\kappa_{bulk} = 0.1119$ Ω^{-1} cm^{-1} at 25 °C):[22]

$$r_1 = \frac{19}{R_p} \qquad (3)$$

The dominant source of error propagated in using eq 3 is introduced into the measurement of θ (±1^o), which produces an approximate relative uncertainty of 10% in r_1.

(20) (a) Wang, G.; Zhang, B.; Wayment, J. R.; Harris, J. M.; White, H. S. *J. Am. Chem. Soc*., in press, 2006. (b) Zhang, Y.; Zhang, B.; White, H. S. *J. Phys. Chem. B* **2006**, *110*, 1768. (c) Zhang, B.; Zhang, Y.; White, H. S. *Anal. Chem.* **2006**, *78*, 477. (d) Zhang, B.; Zhang, Y.; White, H. S. *Anal. Chem.* **2004**, *76*, 6229.
(21) Kuwana, T.; Bubitz, D. E.; Hoh, G. *J. Am. Chem. Soc.* **1960**, *82*, 5811.
(22) (a) Kroner, R. C. *J. Assoc. Off. Anal. Chem.* **1973**, *56*, 295. (b) Pratt, K. W.; Koch, W.f.; Wu, Y. C.; Berezansky *Pure Appl. Chem*. **2001**, *73*, 1783.

Deposition of the POPC Bilayer Membrane. Glass nanopore capillaries were initially cleaned with ethanol, water, and 70% HNO_3/H_2O, followed by a final rinse with copious amounts of water. Prior to deposition of a lipid bilayer, the $i-V$ curve for each glass nanopore capillary was recorded in an aqueous solution containing 1 M KCl and 10 mM phosphate-buffered saline (PBS) adjusted to pH 7.4. Between experiments, glass nanopore capillaries were stored in the same buffer solution.

A "tip-dip" procedure was used to prepare bilayers on the glass nanopore membrane. The conductance cell (~4 mL total volume) was partially filled with the aqueous KCl/PBS (pH 7.4) solution to be used in the $i-V$ measurement. A solution of 2 mg/mL POPC dissolved in chloroform was then carefully injected into the bottom of the cell. A clean glass nanopore capillary is introduced into the upper aqueous phase and slowly pushed through the aqueous/organic interface, keeping the glass nanopore membrane surface parallel to the interface. This step results in the deposition of a lipid monolayer layer across the glass surface. The glass nanopore capillary is then tilted at a ~45° angle and slowly brought back through the interface, depositing the outer layer of the lipid bilayer. The glass nanopore capillary, now covered by a POPC bilayer and in the aqueous solution, was employed in the electrical measurements. The POPC bilayer was removed by immersing the glass nanopore in ethanol, followed by rinsing with water, 70% HNO_3/H_2O, and water as described above.

FRAP Measurements. The formation of a bilayer using the tip-dip method was verified by fluorescence microscopy using an inverted epifluorescence Nikon Eclipse TE 2000-U microscope equipped with a Sensys CCD camera (Photometrics, Roper Scientific). Diffusion coefficients and mobile fractions of the lipids were measured using the fluorescence recovery after photobleaching (FRAP) technique performed on the capillary membrane. Here, the surface-bound fluorescently labeled lipids were bleached momentarily with a laser beam from a 2.5 W mixed gas Ar^+/Kr^+ laser (Stabilite 2018, Spectra Physics). Samples were irradiated at 568.2 nm with 100 mW of power for several seconds. The beam width at half-maximum yielded a bleach spot of ~17 μm after focusing the light onto the bilayer through a 10× objective. The recovery of the photobleached spot was measured as a function of time using time-lapse imaging and subsequently processed using MetaMorph software (Universal Imaging). The fluorescence intensity of the bleached spot was determined after background subtraction and normalization for each image. Using standard procedures,[23] the diffusion coefficient of the dye-labeled lipids was determined. Briefly, the fluorescence recovery as a function of time is fit with a single-exponential equation from which we obtain the mobile fraction of the dye-labeled lipids and the half-time of recovery ($t_{1/2}$). The diffusion coefficient, D, is then calculated from the following equation

$$D = \frac{w^2}{4t_{1/2}}\gamma \tag{4}$$

where w is the full width at half-maximum of the Gaussian profile of the focused beam and γ is a correction factor that depends on the bleaching time and geometry of the laser beam.[23]

***i*−*V* Measurements.** A Dagan Chem-Clamp voltammeter/amperometer (Minneapolis, MN) was employed to record $i-V$ data. A voltage was applied between two Ag/AgCl electrodes, one positioned inside the capillary and one in the external solution. Voltage is always referenced to the electrode inside the capillary. $i-V$ data were acquired at a scan rate of 20 mV/s over the voltage range from −100 to +100 mV. All $i-V$ measurements employed identical internal and external electrolyte solutions.

Preparation of KCl/PBS Solutions. A 1 M KCl/10 mM PBS (pH 7.4) stock solution was used to prepare all other solutions by serial dilution. The diluted solutions are identified throughout the article by their respective KCl concentrations. Thus, a 0.01 M KCl solution corresponds to an aqueous solution containing 0.01 M KCl and 0.1 mM PBS. The contributions of KH_2PO_4 and K_2HPO_4 to the solution conductivity were ignored because these species contribute only ca. 2% to the total ionic strength of all solutions. This error is significantly smaller than other sources of error incurred in computing conductivities from the $i-V$ data.

Results and Discussion

Measurement of the Conductance of the Aqueous Layer. The resistance of the glass membrane containing a single nanopore on which a lipid bilayer is deposited comprises two parts: (1) the resistance of the conical-shaped pore and (2) the resistance of the aqueous layer between the lipid bilayer and the glass support. As described in the Experimental Section, the resistance of a conical-shaped pore that has a length much greater than its radius is determined only by the half-cone angle of the pore (θ), the orifice radius (r_1), and the conductivity of the aqueous solution that fills the pore. Because the pore is fabricated in glass, the negative surface charge on the pore walls can influence the ion concentration within the pore. However, when r_1 is much greater than the Debye length of the solution, λ, the conductivity of the solution in the pore can be assumed to be equal to that of the bulk solution in which it is immersed.[24] This condition is met in our experiments except when using very small nanopores and low KCl concentrations, as described later. Specifically, the orifice radii of the pores used here ranged from 45 to 480 nm, considerably larger than the Debye length of a 1 M KCl solution ($\lambda \approx 0.3$ nm). Thus, it is reasonable to assume that the conductivity of the aqueous solution in the pore corresponds to that of the bulk solution. Under these conditions, the resistance of the pore is given by eq 5.

$$R_p = (\kappa_{bulk} r_1 \pi \tan\theta)^{-1} \tag{5}$$

(Note that the term in eq 2 corresponding to the spreading resistance of the pore exit ($^1/_4$) is omitted in writing eq 5 because this current path no longer exists when a bilayer is deposited across the pore opening).

The resistance of the aqueous layer between the bilayer and glass support is associated with the radially outward (or inward when the voltage polarity is reversed) migration of ions between the pore orifice and the edge of the lipid bilayer film. Assuming that the lipid bilayer extends radially to a distance, r_2, from the center of the pore (Figure 2a), the geometry of the aqueous layer through which charge flows corresponds to that of the annulus region between two concentric cylinders. The resistance of this layer is thus given by eq 6[25]

$$R_d = \frac{\ln(r_2/r_1)}{2\pi\kappa_d d} \tag{6}$$

where d and κ_d are the thickness and ionic conductivity, respectively, of the aqueous layer between the lipid bilayer and the glass support. The total resistance, R_m, obtained from the inverse of the slope of $i-V$ curves of a bilayer-covered glass membrane is thus equal to the sum of R_p (eq 5) and R_d (eq 6). Thus, the value of R_d can be obtained by subtracting R_p from the total resistance ($R_d = R_m - R_p$). However, we show below that R_p is always negligibly small relative to R_m and thus can be ignored (i.e., $R_d = R_m$).

The logarithmic dependence of R_d on the ratio r_2/r_1 greatly reduces the magnitude of the error propagated by uncertainties

(23) Axelrod, D.; Koppel, D. E.; Schlessinger, J.; Elson, E.; Webb, W. W. *Biophys. J.* **1976**, *16*, 1055.

(24) Probstein, R. F. *Physicochemical Hydrodynamics: An Introduction*; Butterworths: New York, 1989.

(25) Chapman, A. J. *Fundamentals of Heat Transfer*; Macmillan Publishing Co.: New York, 1987.

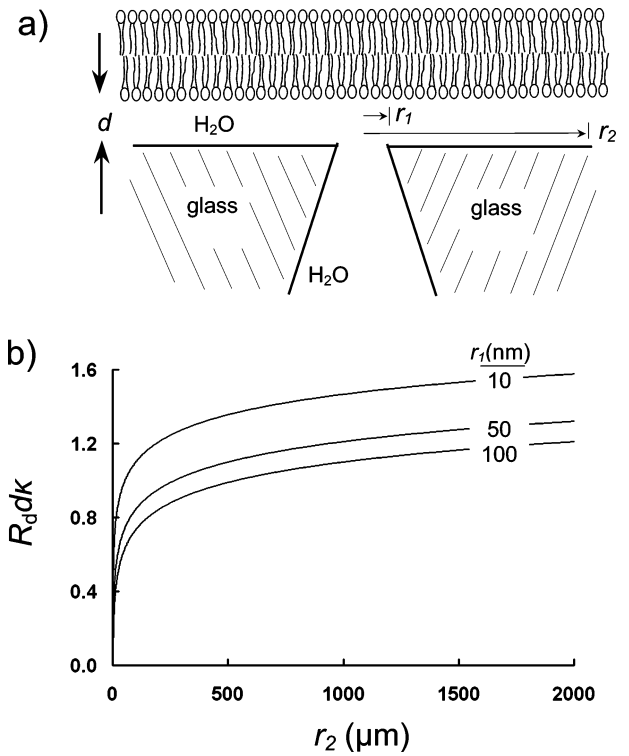

Figure 2. (a) Cross-sectional view of the nanopore/lipid bilayer membrane illustrating the geometry used to analyze the measured resistance. r_1, r_2, and d are the nanopore radius, the radial distance from the pore center, and the water layer thickness, respectively. (b) Plot of normalized resistance, $R_d d\kappa$ (dimensionless) as a function of the distance from the center of the pore (r_2) for $r_1 = 10$, 50, and 100 nm.

in the values of r_2 and r_1. This is quantified in Figure 2b, which shows a plot of the dimensionless group $R_d d\kappa_d$ as functions of r_1 (10 to 100 nm) and r_2 (0 to 2000 μm). An inspection of Figure 2b suggests that $R_d d\kappa_d$ is insensitive to small errors in r_1 and r_2 as long as r_2 is greater than $\sim$100 μm. In the experiments described below, r_1 is known to within 10% as previously discussed. A lipid bilayer film is deposited across the entire surface of a 1000-μm-radius circular glass membrane at the end of the capillary. Thus, the measured value of R_d is relatively independent of the precise value of r_2. For instance, when using $r_1 = 50$ nm, $R_d d\kappa_d$ increases by only 30% (3.80 to 4.95) for an order of magnitude change in r_2 from 100 to 1000 μm. We use $r_2 = 200$ μm throughout the remainder of the article. A caveat in this analysis is that the lipid bilayer is not perfectly formed over the glass membrane but contains defects that may shunt the current to the contacting solution. A defect positioned close to the pore orifice could possibly lower the measured resistance, leading to an *overestimation* of the aqueous layer conductivity. We return to this issue in the discussion of the fluorescence images described below.

Clearly, the structure of the lipid bilayer at the pore opening depicted in Figure 2 is highly idealized. However, because the resistance of the aqueous layer between the glass support and lipid bilayer is so large, we do not anticipate that departures from an idealized flat bilayer structure spanning the pore opening (e.g., lipid remnants inside the pore) have a significant influence on the measured resistance.

***i*−*V* Measurements in 1 M KCl Solutions.** Figure 3 shows typical $i-V$ curves recorded for a glass membrane containing a single nanopore (without lipid bilayer) and the same membrane after the deposition of a POPC bilayer. The radius of the pore opening in this membrane was 84 nm. An inspection of Figure

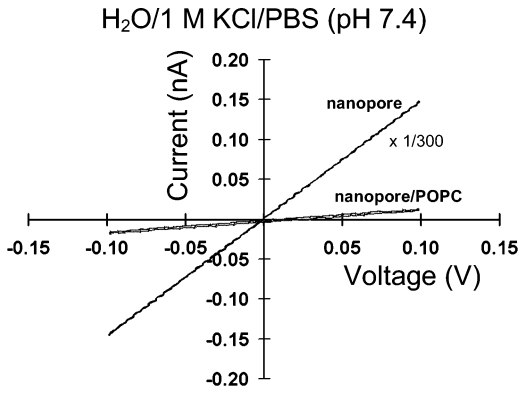

Figure 3. $i-V$ response of an 84-nm-radius pore in 1 M KCl/10 mM PBS buffer (pH 7.4) before (black line) and after (grey line) deposition on a POPC bilayer membrane on the glass surface. The bare pore response is scaled by $^1/_{300}$. The voltage is referenced to the electrode inside the capillary. The $i-V$ responses for the bare and membrane-covered nanopores correspond to resistances of 2.3 MΩ and 6.9 GΩ.

3 indicates that the current through the open pore is ca. 3 orders of magnitude *larger* than that measured after the deposition of the bilayer. Thus, as discussed above, the resistance of the pore containing 1 M KCl, R_p, is negligibly small in comparison to R_m and can be ignored in analyzing the data for the lipid bilayer-covered glass membrane.

From the data presented in Figure 3, the resistance of the glass membrane after deposition of the POPC bilayer is 6.9 GΩ. Assuming a thickness of 1 nm for the aqueous layer and using $r_1 = 84$ nm and $r_2 = 200$ μm, we compute a value of $\kappa_d = 0.0018$ Ω^{-1}cm^{-1}. This value is approximately a factor of 62 smaller than the bulk conductivity of the 1 M KCl solution in which the measurement is made (0.1119 Ω^{-1} cm^{-1}).[22] Table 1 lists results of measurements in 1 M KCl using nine different glass nanopore membranes with pore radii ranging from 45 to 480 nm, which yield an averaged value of $\kappa_d = 0.0026 \pm 0.0006$ Ω^{-1} cm^{-1}. We reiterate that this value assumes a 1-nm-thick aqueous layer thickness and does not include the uncertainty in the literature values of d. Prior to presenting a discussion of the significance and interpretation of κ_d, it is necessary to consider the influence of defects in the film on the measured resistance and the resulting value of κ_d. In the next section, fluorescence images and FRAP experiments are presented that address the role of structure (including possible defects) and the fluidity of the POPC bilayers used in these experiments.

Fluorescence Images and FRAP. Figure 4 shows a typical FRAP curve for the recovery of fluorescence as a function of time, fit to a single-exponential curve. The inset shows images of the glass membrane surface immediately after bleaching with the laser beam (circled regions indicate the location of the bleached spot) and then after the bleached area has recovered. The diffusion coefficient was obtained over many different areas of the membrane surface and averaged, yielding a value of 3.6 ± 0.6 μm^2/s. The percentage of mobile lipids was determined over each area and found to be 90 ± 1% on average for a given electrode. On occasion, certain areas deviated from this value. The highest mobile fraction that we obtained was 97%, and the lowest value was 78%. We attribute this observed spread to variations in surface roughness, which is a result of the polishing and preparation procedures that can vary from membrane to membrane and even within different regions of a given membrane. Although these slight differences in surface preparation are easily observed because of their effect on the mobile fraction of lipids during FRAP experiments, we anticipate that small immobile

Table 1. Aqueous Layer Conductivity (κ_d) in 1 M KCl/PBS (pH 7.4)

radius, r_1 (nm)	nanopore resistance (MΩ)	nanopore/bilayer resistance (GΩ)	conductivity, κ_d[a] (Ω^{-1} cm^{-1})
84[b]	2.26	6.93	0.0018
84	2.26	6.20	0.0020
84	2.26	5.68	0.0022
84	2.26	6.03	0.0021
190	1.00	5.19	0.0021
190	1.00	6.50	0.0017
190	1.00	5.26	0.0021
190	1.00	1.71	0.0065
59	3.23	2.23	0.0058
52	3.66	1.85	0.0071
475	0.40	2.82	0.0034
475	0.40	3.05	0.0032
475	0.40	8.31	0.0012
475	0.40	3.74	0.0026
475	0.40	3.62	0.0027
78	2.43	6.51	0.0019
78	2.43	7.28	0.0017
78	2.43	7.63	0.0016
90	2.12	6.14	0.0020
90	2.12	6.93	0.0018
90	2.12	6.57	0.0019
45	4.20	7.15	0.0019
45	4.20	3.07	0.0044
45	4.20	3.80	0.0035
261	0.73	5.75	0.0018
261	0.73	7.17	0.0015
261	0.73	5.56	0.0019
			average: 0.0026 ± 0.0006 Ω^{-1} cm^{-1}

[a] Calculated assuming $d = 1.0$ nm and $r_2 = 0.2$ mm. [b] Between repetitions using the same glass nanopore membrane, the POPC bilayer was removed by soaking the membrane in ethanol, rinsing with ultrapure water, and then rinsing with 70% HNO_3/H_2O, which is followed by rinsing with copious amounts of ultrapure water.

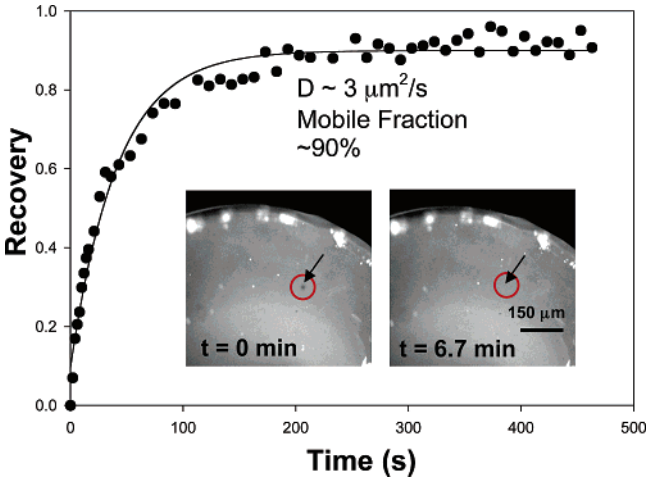

Figure 4. Typical FRAP curve of fluorescence recovery as a function of time for a POPC lipid bilayer on a glass nanopore membrane surface. The data are fit with a single-exponential curve (solid line), from which $t_{1/2}$ and the diffusion coefficient, D, are obtained. The mobile fraction is determined as the ratio of the fluorescence level at $t = \infty$ to the corresponding value prior to bleaching. The inset shows a representative set of images of a membrane surface immediately after bleaching and then at recovery. The circled regions indicate the location of the bleached spot in the images.

fractions of lipids have a relatively small effect on the conductance measurements and the ability to form a high resistance seal.

Dependence of κ_d on Bulk KCl Concentration. The average value of κ_d measured in a 1 M KCl/10 mM PBS (pH 7.4) solution (0.0026 ± 0.0006 Ω^{-1} cm^{-1}) is approximately 43 times smaller than the corresponding conductivity of the bulk solution in which the measurement is made. This finding indicates that the concentration and/or the mobility of the charge-carrying ions between the POPC bilayer and the glass surface is significantly lower than that of the bulk solution.

Because glass is negatively charged at pH 7.4, we assume that the predominant charge-carrying ion is K^+, a consequence of Cl^- being electrostatically excluded from the narrow layer of aqueous solution. Our experiments, however, do not provide direct evidence to support this hypothesis. However, because the POPC bilayer is electrically neutral, it is reasonable to anticipate that the surface concentration of K^+ is approximately equal to the anion surface charge density, σ^s, resulting from deprotonation of the silanol groups. On fused quartz surfaces, σ^s is reported to be ~1 negative charge per nm^2 at neutral pH.[26] Although this value may differ at the glass membrane surface, it serves as a guide in estimating the anticipated surface concentration of K^+. Thus, following this simple line of reasoning, the surface coverage is anticipated to be ~1 K^+ per nm^2 and independent of the concentration of KCl in the bulk solution. The independence of the surface concentration of K^+ on bulk KCl concentration is supported by vibrational sum frequency spectra of H_2O in the layer between fused quartz and lipid bilayers, which are weakly dependent on the concentration of the bulk NaCl.[27]

To explore this line of reasoning, the $i-V$ responses of three glass nanopore membranes, onto which POPC bilayers were deposited, were recorded as a function of the bulk KCl concentration over the range of 10^{-4} to 1 M. Figure 5 shows $i-V$ curves for a glass membrane containing a single nanopore with a 59 nm radius orifice as a function of KCl concentration. In this set of experiments, all solutions were prepared from the stock 1 M KCl/10 mM PBS solution by serial dilution. For the example data shown in Figure 5, ohmic $i-V$ behavior was observed for the open nanopore in 1 M KCl solutions. As the KCl concentration was decreased, pronounced current rectification was observed, with the current being slightly larger when positive current passed from the internal solution to the external solution. Less rectification was observed when using larger nanopores. These observations are in good qualitative agreement with the original report by Wei et al. of current rectification in tapered glass capillaries[28] and are a consequence of the interaction of the charge-carrying ions with the negatively charged glass surface.[28,29] In contrast, ohmic $i-V$ behavior was always observed after POPC deposition on the glass membrane nanopore at all KCl concentrations.

Table 2 and Figure 6 summarize experimental measurements of the dependence of R_d and κ_d on bulk KCl concentration for three glass membrane nanopores ($r_1 = 59$, 84, and 190 nm). In addition to plotting R_d in Figure 6, values of the resistance of the glass membrane prior to POPC bilayer deposition, R_p, are also included for comparison. The straight lines plotted on top of the latter values are theoretical values based on the nanopore geometry and literature values of the conductivity of KCl solutions.[22] (As noted in the Experimental Section, the small contributions of the buffer electrolytes, KH_2PO_4 and K_2HPO_4, to the bulk ion conductivity (~2%) are ignored.) Good agreement is obtained between the predicted and measured values of R_p, except at the lowest KCl concentrations (10^{-3} and 10^{-4} M) where the measured values are significantly lower than predicted. The

(26) Ong, S.; Zhao, X.; Eisenthal, K. B. *Chem. Phys. Lett.* **1992**, *191*, 327.
(27) Kim, J.; Kim, G.; Cremer, P. S. *Langmuir* **2001**, *17*, 7255.
(28) Wei, C.; Bard, A. J.; Feldberg, S. W. *Anal. Chem.* **1997**, *69*, 4627.
(29) (a) Siwy, Z.; Gu, Y.; Spohr, H. A.; Baur, D.; Wolf-Reber, Spohr, R.; Apel, P.; Korchev, Y. E. *Europhys. Lett.* **2002**, *60*, 349. (b) Fulinski, A.; Kosinska, I.; Siwy, Z. *New J. Phys.* **2005**, *7*, 132.

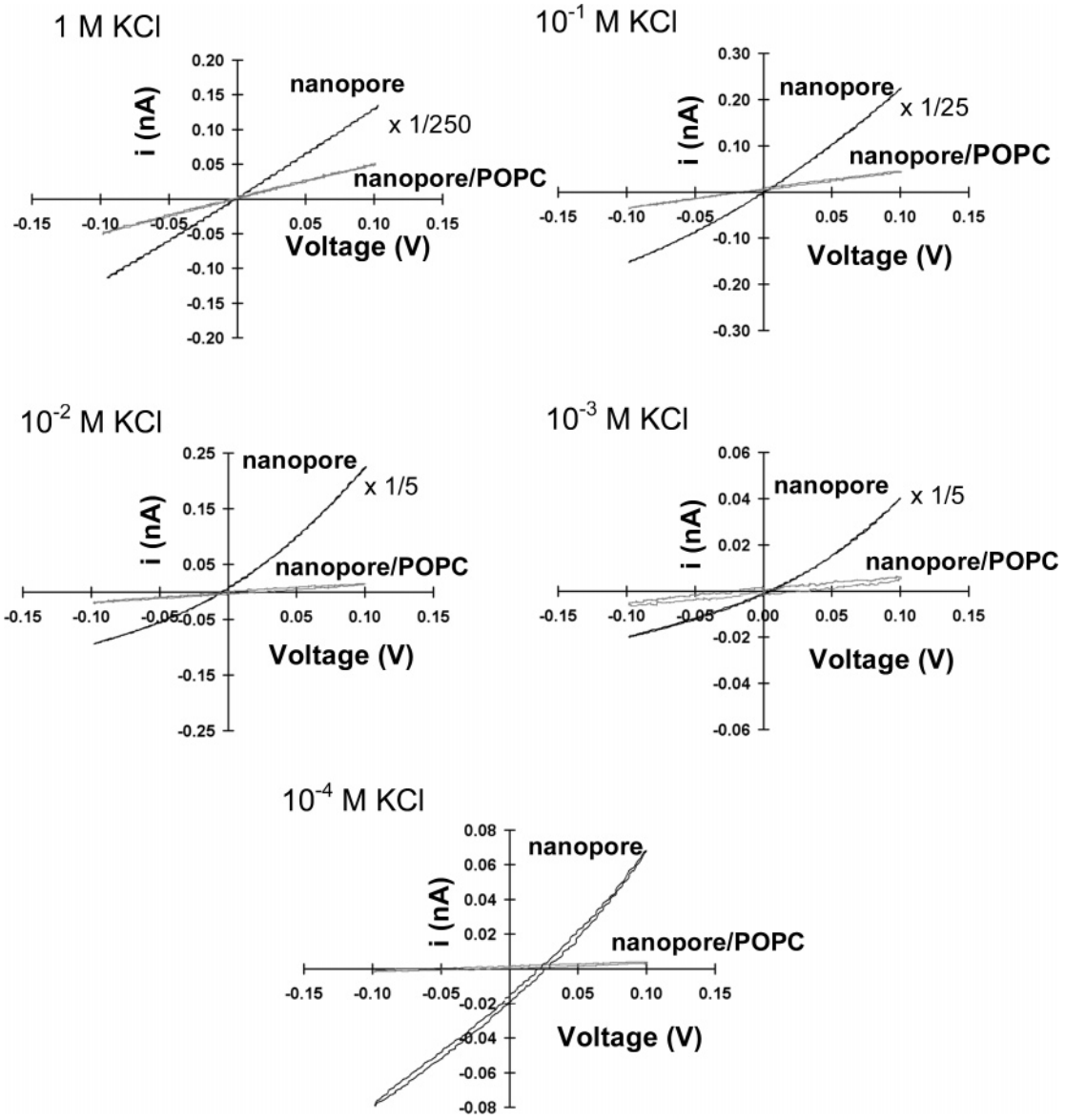

Figure 5. $i-V$ responses of a 59-nm-radius nanopore before (black lines) and after (grey lines) deposition on a POPC bilayer membrane on the glass surface as a function of the KCl/PBS concentration in the contacting solutions. (Note that the $i-V$ responses of the bare nanopore are scaled differently to fit onto the plots.) The voltage is referenced to the electrode inside the capillary. The $i-V$ responses for the bare and membrane-covered nanopore correspond, respectively, to resistances of 3.2, 21, 130, 690, and 1400 MΩ and 2.2, 2.5, 5.9, 19, and 40 GΩ.

divergence of predicted and measured values of R_p for nanopores at low concentrations is related to the current rectification discussed above and is well understood to be a consequence of the electric field originating at the charged glass surface.[24,30,31] This field extends over a significant fraction of the pore diameter at low KCl concentrations, regulating and maintaining the pore conductivity at a nearly fixed value, as demonstrated recently by several groups in investigations of ionic conductivity in nanofluidic channels.[32] In our experiments, the Debye length is ∼30 nm in a 10^{-4} M KCl solution, which is a significant fraction of the radius of the smaller pores. Thus, K^+ is the predominant ionic species at the small end of the conically shaped pore at low KCl concentrations and is maintained at a concentration required to electrically balance the negative charge on the pore wall.[24,30,32]

The data plotted in Figure 6 clearly demonstrate that the ionic resistance between the POPC bilayer and the glass surface is constant between 1 and 10^{-2} M KCl, increasing very slightly at concentrations between 10^{-3} and 10^{-4} M. The nearly constant value of R_d over a 4 orders of magnitude change in KCl concentration is remarkable. Assuming that the thickness of the intervening aqueous layer between the POPC bilayer and glass surface does not vary significantly as a function of bulk KCl concentration, this finding directly indicates that κ_d is essentially

(30) (a) Revil, A.; Glover, P. W. J. *Phys. Rev. B* **1997**, *55*, 1757. (b) Revil, A.; Glover, P. W. J. *Geophys. Res. Lett.* **1998**, *25*, 691.

(31) Reference 30 presents an excellent discussion of the importance of electrical double-layer conductivity in small-diameter pores and porous materials at low electrolyte concentrations as well as a description of research on this topic beginning in the 1950s.

(32) (a) Stein, D.; M. Kruithof, M.; Dekker, C. *Phys. Rev. Lett.* **2004**, *93*, 035901-1-4. (b) Petersen, N. J.; Dutta, D.; Alarie, J. P.; Ramsey, J. M. Proceedings of the 8th International Conference on Miniaturized Systems in Chemistry and Life Sciences; Laurell, T., Nilsson, J., Jensen, K., Harrison, D. J., Kutter, J. P. Eds.; Royal Society of Chemistry: Cambridge, U.K., 2004; Vol. 1, p 348. (c) Petersen, N. J.; Ramsey, J. M., Proceedings of the 9th International Conference on Miniaturized Systems in Chemistry and Life Sciences; Jensen, K., Han, J., Harrison, D. J., Voldman, J., Eds.; Transducers Research Foundation: San Diego, CA, 2005; pp 1252−1254. (d) Fan, R.; Karnik, R.; Yue, M.; Majumdar, A.; Yang, P. *Phys. Rev. Lett.* **2005**, *95*, 086607. (e) Goldberger, J.; Fan, R.; Yang, P. *Acc. Chem. Res.* **2006**, *39*, 239. (f) Karnik, R.; Fan, R.; Yue, M.; Li, D.; Yang, P.; Majumdar, A. *Nano Lett.* **2005**, *5*, 943. (g) Fa, K.; Tulock, J. J.; Sweedler, J. V.; Bohn, P. W. *J. Am. Chem. Soc.* **2005**, *127*, 13928.

Table 2. Aqueous Layer Conductivity (κ_d) as a Function of [KCl]

pore radius, r_1 (nm)	[KCl][a]	nanopore resistance (MΩ)	nanopore/bilayer resistance (GΩ)	κ_d[b] (Ω^{-1} cm^{-1})
84	10^0	2.26	6.93	0.0018
	10^{-1}	18.9	6.61	0.0019
	10^{-2}	200	6.91	0.0018
	10^{-3}	1138	15.3	0.00081
	10^{-4}	1567	15.9	0.00078
190	10^0	1.00	5.19	0.0021
	10^{-1}	8.83	8.86	0.0013
	10^{-2}	79.9	4.61	0.0024
	10^{-3}	458	30.0	0.00037
	10^{-4}	2060	35.6	0.00031
59	10^0	3.23	2.23	0.0058
	10^{-1}	21.2	2.52	0.0051
	10^{-2}	117	5.94	0.0022
	10^{-3}	693	18.6	0.00070
	10^{-4}	1400	40.6	0.00032

[a] The stock 1 M KCl/10 mM PBS solution was diluted 10-fold in successive steps to yield the indicated concentrations. [b] Calculated assuming $d = 1.0$ nm and $r_2 = 0.2$ mm.

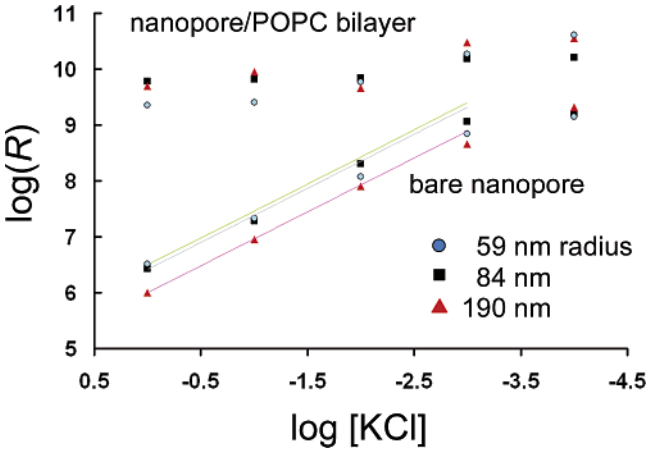

Figure 6. Plot of log(R) (both R_d and R_p) vs log[KCl] for 84-, 190-, and 59-nm-radius nanopores before and after deposition on a POPC bilayer membrane on the glass surface (data from Table 2). The solid lines correspond to computed values of log(R_p) based on the bulk solution conductivity and pore geometry.

independent of the bulk KCl concentration because all other factors that enter into computing κ_d using eq 6 are held constant in these measurements.

The independence of κ_d with respect to bulk KCl concentration is consistent with the expectation (vide supra) that current in the aqueous layer is due to the migration of surface counterions that are present in order to maintain a nearly electrically neutral surface. Thus, κ_d reflects the product of the concentration and the mobility of K^+ and can be expressed as

$$\kappa_d = \frac{F\Gamma^+\mu^+}{d} \qquad (7)$$

where Γ^+ and μ^+ are the surface concentration and electrical mobility of K^+, respectively. Taking Γ^+ as being approximately equal to density of negative surface sites ($\sigma^s \approx 1/\text{nm}^2$), we computed μ^+ from eq 7 to be 2.1×10^{-5} cm^2/Vs. We note that a value of Γ^+ equal to 1 K^+/nm^2 contained within a 1-nm-thick aqueous layer corresponds to ~1 M K^+. For comparison, the ion mobility of K^+ in a 1 M KCl solution is $\sim 6 \times 10^{-4}$ cm^2/Vs. Whereas our value of μ^+ is a rough estimate, the mobility of K^+ in the aqueous layer between the POPC bilayer and glass appears to be significantly lower than in free solution. Ho et al. reported a similar decrease in ionic mobility within a nanometer-diameter pore in silicon nitride (SiN), a consequence of strong interactions between the charged SiN pore wall and charge-carrying ions.[33]

An alternative explanation for the lack of a strong dependence of κ_d on bulk KCl concentration is that both Γ^+ and μ^+ vary but in a manner that offsets each other to yield a constant-valued κ_d. Although we cannot eliminate this possibility, this would require a mechanism by which the variation in μ^+ is inversely proportional to the variation in Γ^+. For this reason, we believe that the constancy of κ_d reflects the fact that Γ^+ is independent of bulk KCl concentration.

Conclusions

We have presented a relatively straightforward method using the glass membrane nanopore that allows the measurement of the conductivity of the aqueous layer between a lipid bilayer film and a glass support. The methodology may be readily extended to different types of lipid bilayer structures and solution conditions and should thus prove to be a versatile means to directly measure the in-plane electrical properties of the confined aqueous layer. In turn, electrical measurements of the type described above should yield additional fundamental information about the structure and dynamics of ions and solvent molecules confined to a narrow layer.

The conductivity of the aqueous layer between a POPC bilayer and glass is nearly independent of the concentration of bulk KCl. This result strongly suggests that the concentration of charge-carrying K^+ is set at a fixed value determined by the surface density of surface anionic sites, a result that is analogous to the fixed concentration of charge-carrying ions within charged nanopores at low ion concentration (also observed in the above studies). Further investigations are required to unravel the dependence of the conductivity on the chemical composition and the mobility of ions within the aqueous layer.

Acknowledgment. This research was supported by the Defense Advanced Research Project Agency (FA9550-06-C-0006 and FA9550-06-C-000C). S.D. thanks Dr. Fernando Albertorio for his assistance with the FRAP measurements and valuable discussions.

LA061457A

(33) Ho, C.; Qiao, R.; Chatterjee, A.; Timp, R. J.; Aluru, N. R.; Timp, G. *Proc. Natl. Acad. Sci. U.S.A.* **2005**, *102*, 10445.